

*Special Issue: Artificial Intelligence*

*Scientific Paper*

Doi: <http://dx.doi.org/10.1590/1809-4430-Eng.Agric.v43nepe20210164/2023>

## LOW-COST IRRIGATION MANAGEMENT SYSTEM: IMPROVING DATA CONFIDENCE THROUGH ARTIFICIAL INTELLIGENCE

Thiago A. C. da Cruz<sup>1\*</sup>, Patricia A. A. Marques<sup>1</sup>

<sup>1\*</sup>Corresponding author. University of São Paulo/Piracicaba - SP, Brazil.

E-mail: [thiagoalberto@usp.br](mailto:thiagoalberto@usp.br) | ORCID ID: <https://orcid.org/0000-0003-4918-2020>

### KEYWORDS

efficient irrigation, artificial neural networks, weather station, low-cost equipment.

### ABSTRACT

A common scenario in the developing countries is the low income and less education of producers. Thus, the tools used for irrigation management must be cheap and easy to handle. In this work, an autonomous and low-cost network of micro-weather stations has been developed for irrigation management. Simulations were performed to evaluate the ability of intelligent systems to compute evapotranspiration with noisy and insufficient data. The network of micro-weather stations was then applied to autonomous irrigation management of a crop of bell peppers. Statistical analysis was performed on data from the developed system and a standard weather station. The results show no statistical difference between the values of evapotranspiration calculated with data from these two sources. The developed system performed with a coefficient of determination of 0.968, mean absolute error of 0.055 mm day<sup>-1</sup>, and root mean square error of 0.063 mm day<sup>-1</sup>. The study shows that low-cost intelligent systems can be used as viable tools for efficient irrigation management.

### INTRODUCTION

Growing disputes over water access have increased the need for technologies that reduce the use of this resource (FAO & WWC, 2015). Suitable irrigation management leads to productivity gains with reduced water use (Sidhua et al., 2021; Poggi et al., 2021). However, this requires techniques and equipment that are recommended by the FAO in Irrigation and Drainage Paper 56 (Allen et al., 1998). Moreover, proper measures should be taken so that the socioeconomic plurality of the involved agents does not appear as an obstacle for the financial cost and operability of the equipment and techniques (Zhang et al., 2021). Even though the agro-industrial market of Brazil represents more than 20% of its gross domestic product (Oliveira, 2016), such techniques and equipment are unfeasible for most rural producers in the country. The 2006 agricultural census (IBGE, 2009) showed that 85.4% of the agricultural establishments belong to small producers and that, of all properties, only 5.8% have a monthly net family income

above 4083.00 Brazilian reais (BRL). The preliminary results of the 2017 census indicated that 23% of the rural producers are 65 years of age or older and that 22.9% of all producers do not know how to read and write.

One way to avoid the above obstacles is the development of low-cost weather stations that can automatically calculate the reference evapotranspiration (ET<sub>0</sub>), determine the crop coefficient, and activate irrigation pumps and valves (Jimenez et al., 2020). The variables that influence evapotranspiration interact with each other in a complex and nonlinear manner, and low-cost sensors often have a close relationship between noise and the signal of interest. In addition, the instrument response often shows high nonlinearity (Curto et al., 2018, Guo et al., 2018, Castell et al. 2017, Leal-Junior et al., 2018, Johnson et al., 2018). Thus, one approach to estimating ET<sub>0</sub> is by using a universal function approximator (Kosko, 1994) based on an artificial neural network (ANN) (Antonopoulos & Antonopoulos, 2017). Kumar et al. (2002) evaluated the

<sup>1</sup> University of São Paulo/Piracicaba - SP, Brazil

Area Editor: Rouverson Pereira da Silva

Received in: 8-31-2021

Accepted in: 12-21-2022



performance of several ANNs at estimating  $ET_0$  around the meteorological station California Irrigation Management Information System, Davis, California. They tested several topologies with different numbers of neurons and hidden layers as well as various learning algorithms against the Penman–Monteith (PM) method. Two datasets were used in their study. The first set (January 1, 1990–June 30, 2000) contained only meteorological data, which were used to train the ANN to estimate  $ET_0$ . Whereas the second one (January 1, 1960–December 31, 1963) included both meteorological data and data from a weighing lysimeter that was installed under a grass field. Thus, the  $ET_0$  estimation by the ANN and PM method could be compared against the data from the weighing lysimeter. The topology with the best result exhibited a lower estimation error than the PM method for all learning algorithms. Trajkovic (2005) used daily data from seven Serbian weather stations from 1971 to 1996 to analyze the  $ET_0$  estimation performances of four temperature-based models: Thornthwaite (Thornthwaite, 1948), Hargreaves (Hargreaves & Samani, 1985), reduced PM (Allen et al., 1998), and radial basis function network. They compared the estimations against  $ET_0$  calculated from the FAO-56 PM equation. The radial basis function network demonstrated the best estimation performance for most of the seven locations. Kisi (2006) used an ANN to estimate  $ET_0$  at two weather stations of the California Irrigation Management Information System (CIMIS) using different combinations of weather data from 2001 to 2004: (1) only solar radiation ( $R_s$ ), (2)  $R_s$  and temperature (T), (3)  $R_s$ , T, and relative humidity (RH), and (4)  $R_s$ , T, RH, and wind speed ( $U_2$ ). The ANN with the combination of  $R_s$  and T data showed a better  $ET_0$  estimation than the CIMIS-Penman, Hargreaves & Samani (1985) and Jones & Ritchie (1990) methods for both calibrated and uncalibrated versions.

Many studies have considered the capability of intelligent systems (ISs) at predicting  $ET_0$  as well as the applicability of Internet of Things (IoT) systems to supporting irrigation management (Jimenez et al., 2020; Abioye et al., 2020). However, few studies have considered the capability of ISs to handle low-cost sensors for irrigation management. This study has evaluated the effectiveness of using low-cost sensors with an intelligent system for irrigation management.

## MATERIAL AND METHODS

### Simulations

First, simulations were performed with an ANN and adaptive neuro-fuzzy inference system (ANFIS) to evaluate the ability of an IS to estimate  $ET_0$  using low-cost sensors, which often provide inaccurate, noisy, and insufficient data. The inputs were the meteorological data, and the output was  $ET_0$ . Daily meteorological data (i.e., T, RH,  $R_s$ , and  $U_2$ ) were obtained from the Biosystems Engineering Department of ESALQ/USP automatic weather station (22°42'30" S, 47°38'00" W, 546 m) for January 1, 2001–December 31, 2015. The data were used to generate 5478  $ET_0$  values as calculated by the FAO-56 PM method (Allen et al., 1998) in addition to a dataset of the corresponding daily means for the meteorological data. This automatic weather station belongs to the National Institute of Meteorology and differs from the station used in later experiments. The dataset was divided into three sets: training (70%), validation (10%), and test (20%). The data assigned to each set were chosen randomly. Simulations were performed by using the software MATLAB. Thus, the training and validation datasets contributed to the learning of the system. The test dataset was used to evaluate the system performance.

All meteorological data from the automatic weather station were degraded (Raj et al., 2022; Lu et al., 2015; Fang et al., 2021; Alavi et al., 2006; Bedi, 2022; Yu et al., 2022) to mimic possible errors inherent to low-cost equipment. This degradation comprised the following:

1. A proportion factor randomly chosen from the range of 0.1–1.0 was applied to each meteorological variable to emulate the sensitivity of a sensor to meteorological data (FIGURE 1).
2. A threshold was included that shifted the correlation curve up or down by an amount proportional to the maximum variation of the meteorological data in question. The ratio and the slope of the displacement plateau were also randomly chosen. This was to simulate systemic errors in analog-to-digital conversion (FIGURE 2).
3. Random and time-varying noise was added to simulate sensor noise and errors (FIGURE 3). The maximum amplitude for the noise was set to 0%, 5%, 10%, 40%, and 80%.

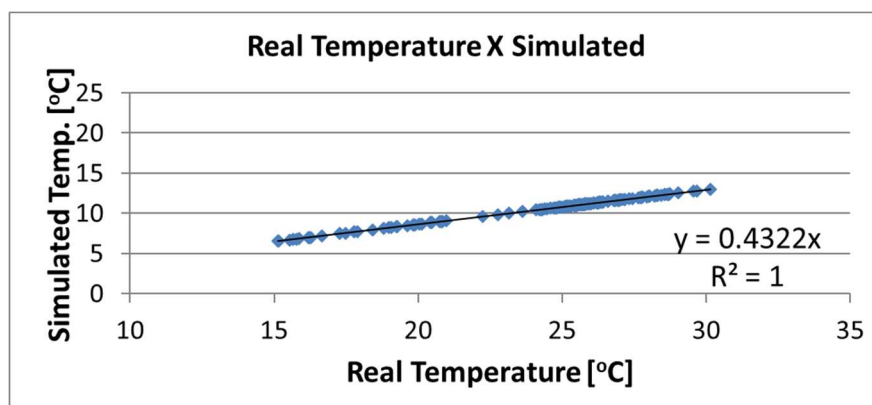


FIGURE 1. Effect of adding a proportion factor to the data provided to the IS. The unaltered data are shown on the left, and the data after application of the proportion factor are shown on the right.

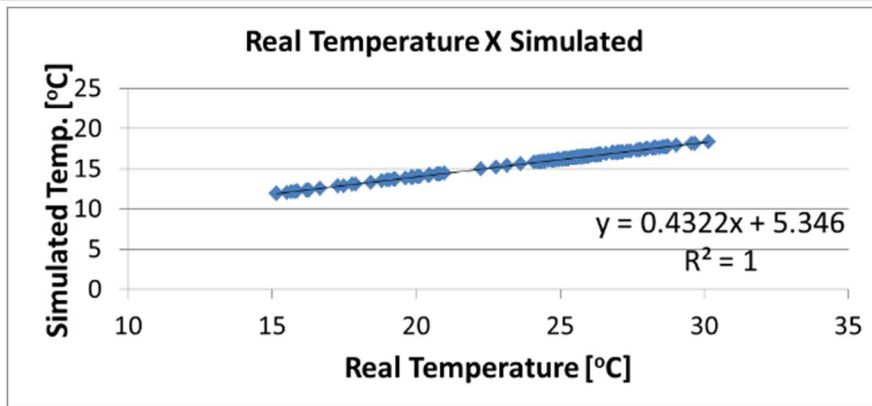


FIGURE 2. Effect of adding a level of deviation to the data provided to the IS. The unaltered data are shown on the left, and the data after application of the proportion factor and displacement plateau are shown on the right.

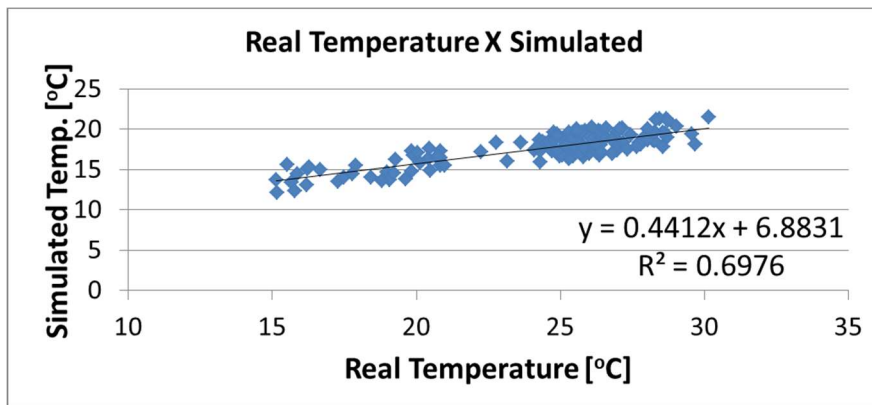


FIGURE 3. Effect of adding time-varying random noise to the data provided to the IS. The unaltered data are shown on the left, and the data after application of the proportion factor, displacement threshold, and time-varying random noise are shown on the right.

The developed ANN had two layers. The hidden layer had three, five, or 10 neurons, a sigmoid activation function, and the Levenberg–Marquardt learning method. The ANFIS inputs were fuzzified with three, five, and seven linguistic variables, and the membership functions of the antecedents followed a Gaussian distribution. The ANN performance with five and 10 neurons and the ANFIS performance with five and seven linguistic variables did not statistically differ from each other. Thus, simulations proceeded with an ANN of five neurons in the hidden layer and ANFIS of five linguistic variables.

Next, the two ISs were evaluated for their  $ET_0$  estimation performance when meteorological data were excluded and the time-variant noise was increased. Changes to the proportion factor and degraded signal threshold did not influence the IS performance, which was evaluated according to the coefficient of determination ( $R^2$ ), mean absolute error (MAE), root mean square error (RMSE), standard deviation ( $\sigma$ ), and proportion factor ( $F_p$ ). The last parameter was used to measure how much the developed model underestimated or overestimated the real data. Once the simulations were completed and the capabilities of the

ISs were elucidated, the developed system was constructed, and experiments were performed as described below.

#### Developed network

The developed network comprised three components: a set of wireless solar-powered micro-weather stations (MWSs), local irrigation servers, and a cloud server. The set of MWSs worked as a sensor network, where each MWS was a node containing multiple sensors. Each local irrigation server stored all data at a node, and it included a graphical user interface so that the user could visualize the status of each node and manually turn the irrigation system on and off. The cloud server stored data from all local irrigation servers. The user could access the farm data through a mobile device if desired.

#### Micro-weather station

Each MWS had sensors to measure T, RH,  $R_s$ , the soil moisture and temperature, the temperature of the electronic circuits, and the battery voltage. In addition, it had a solar panel, a pack of nickel–metal hydride (NiMH) batteries, an XBee radio, an ultralow-power microcontroller, and three printed circuit boards (PCBs) (FIGURE 4 and FIGURE 5).

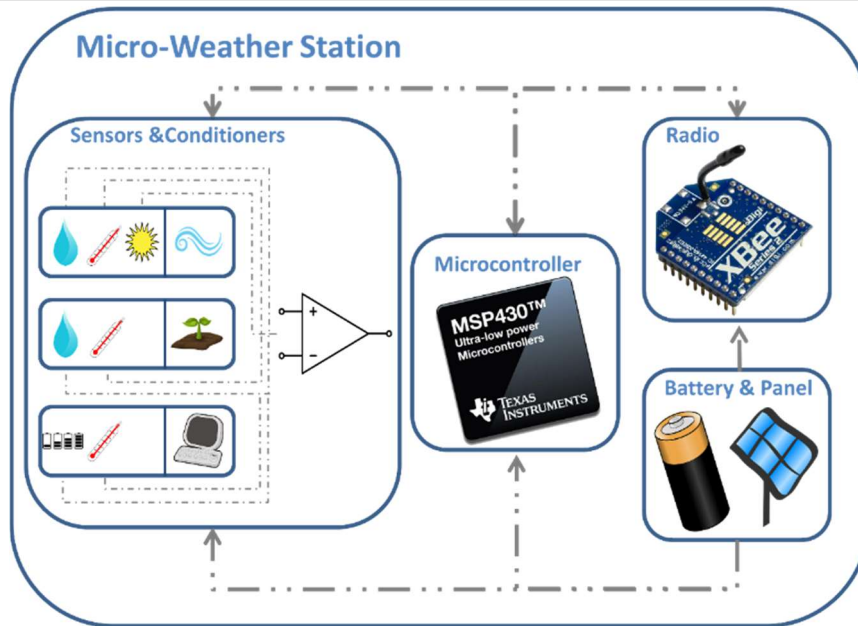


FIGURE 4. Schematic of a micro-weather station (MWS). Each MWS has sensors to measure the air temperature, humidity, soil temperature, moisture, and other parameters. It also has an ultralow-power microcontroller, a radio, a solar panel, and batteries.

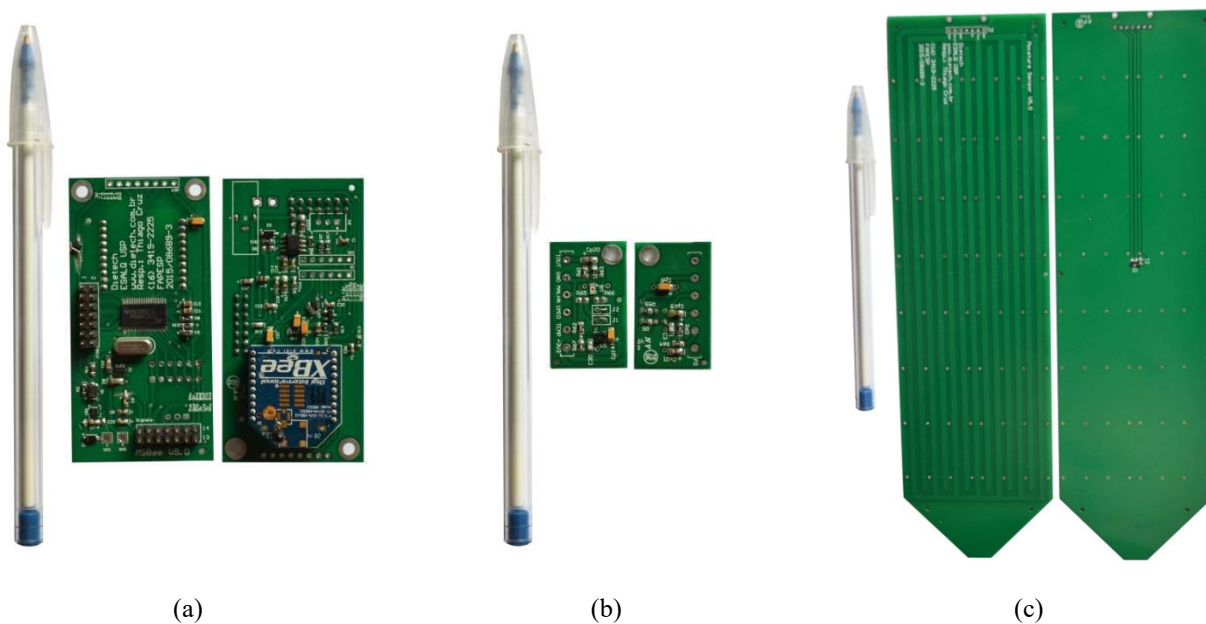


FIGURE 5. Printed circuit boards (PCBs) of a micro-weather station: (a) main PCB (8 cm × 4 cm) containing the microcontroller, radio, and correction circuits; (b) PCB for the weather sensors (4 cm × 2 cm); and (c) PCB for the moisture sensor (25 cm × 7 cm).

An anemometer was not included because the simulation results showed that  $U_2$  made a negligible contribution to the estimated  $ET_0$ . Because the simulation performances of the two ISs did not differ from each other, and the calculations involved in the ANN are more straightforward than the calculations involved in the ANFIS (Binfet & Wilamowski, 2001), the ANN was implemented in the microcontroller of the MWS.

**Embedded artificial neural network**

The embedded ANN (EANN) had the following topology: five neurons in the hidden layer, the sigmoid activation function, and the Levenberg–Marquardt learning method. The inputs were T, RH, and  $R_s$ . The output was

$ET_0$ . To train the EANN, meteorological data from a Campbell Scientific station (CSS) were used to calculate the corresponding  $ET_0$  values, and the dataset was divided into three groups as described above. Then, the learning algorithm was applied in the software MATLAB, and the matrix of synaptic values was embedded in each MWS. Four events were used for training: the first on April 23, followed by events at 14-day intervals until the last one on May 28. All data collected for each event were used.

Note that the CSS differs from the automatic weather station used in the simulations. The CCS was located inside the experimental area, and the automatic weather station was located >500 m from the experimental area.

## Cost analysis

After the ability of the ISs to estimate  $ET_0$  from noisy meteorological data was confirmed, the necessary hardware for construction of the network was developed. Because one of the objectives of this work was to develop and implement a low-cost system, the cost for constructing the developed system was analyzed. Products sold by Digi-Key Electronics, a global distributor of electronic components, that met project specifications were found, and both their unit cost and bulk order cost were obtained. This is because products purchased in large quantities (e.g., 100, 1000, 5000 units) can be obtained at a significantly lower cost. Therefore, if a large number of MWSs is planned for production, the manufacturing costs will be reduced considerably owing to economies of scale. Building one MWS was calculated to cost 71.63 US dollars (USD). Assembling an irrigation server, including peripherals such as the power supply, touchscreen panel, and radio, cost 262.81 USD. The maximum number of MWSs that a single server could manage was not determined; however, the limiting factor should be the processing power of the Raspberry Pi, which would have to simultaneously process a large volume of data. It was estimated that a single server could manage hundreds of MWSs. The cost of manufacturing an MWS together with an irrigation server was less than 400.00 USD, which was equivalent to 2000.00 BRL in mid-August 2021. At this time, meteorological stations were being sold in Brazil at 30,000.00–60,000.00 BRL, depending on the manufacturer and accuracy of the

equipment. Thus, the cost of constructing the developed system was about 15–30 times less than that of purchasing a commercial system. Gunawardena et al. (2018) developed and tested a low-cost system for environmental monitoring that was an order of magnitude cheaper than acquiring a commercial system, which is consistent with the cost analysis in this work.

## Experimental area

The experiment was carried out inside a greenhouse in the Biosystems Engineering Department of the Luiz de Queiroz School of Agriculture of the University of São Paulo (ESALQ/USP) at the Piracicaba–SP campus (22°42'40.67" S, 47.37–46.19" W, 546 m). The greenhouse was 6 m × 18 m with a right foot of 4 m. It was covered by a 150- $\mu$ m-thick transparent polyethylene tarpaulin treated with ultraviolet ray protection. The sides of the greenhouse were coated with an anti-aphid screen and were oriented west–east. According to the Center for Meteorological and Climatic Research Applied to Agriculture (CEPAGRI), the local climate is Cwa as per Köppen's classification, which corresponds to a subtropical dry winter (<18°C) and hot summer (>22°C). FIGURE 6 shows the spatial arrangement of the experiment. The CSS was next to the pots in which bell peppers were planted, which were spaced 0.45 m apart in rows that were 1 m apart. The MWSs were installed in pots 1, 3, 5, 7, 9, 11, 13, 15, 17, and 19, which are denoted as E1, E3, E5, etc. Furthermore, one MWS was installed next to the CSS, which was denoted as E20.

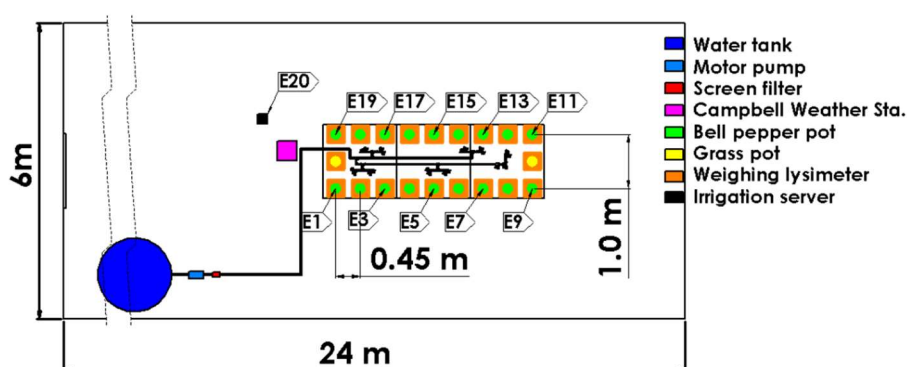


FIGURE 6. Experimental setup (dark blue: 1.000 L water tank, light blue: motor pump, red: screen filter, pink: Campbell Scientific station, orange: weighing lysimeters, green: bell pepper pots, yellow: Bahia grass, black: irrigation server).

The CSS saved data at 15-min intervals. The data logger (CR23X, Campbell Scientific) stored the following variables:  $R_s$ , T, RH, vapor pressure for saturation, current vapor pressure,  $U_2$ , and wind direction. The sensors included HMP45C-L (T and RH), CM3 (silicon pyranometer), and 014A-L (3-cup anemometer).

## Experiment

The bell pepper plants were raised from seedlings from December 15, 2017 to January 24, 2018, after which they were transplanted into pots with dimensions of 35 cm (superior diameter) × 29 cm (inferior diameter) × 35 cm (height). The developed system was installed on April 1, 2018, and it was used to manage the irrigation system starting from April 24. The experiment was carried out until

July 31, 2018. Every day at 8:00 am LT, the motor pump was turned on. After the system pressure was stabilized, the solenoid valves were turned on. Each pot with an MWS was irrigated with the amount calculated using the data from the corresponding MWS. The other pots were irrigated with the amount calculated using data from the CSS. Before April 24, all pots were irrigated according to the data from the CSS.

## Climatic variability

The variability of the greenhouse microclimate was evaluated at 15-min and daily intervals for T and RH. The data were provided by Sensirion SHT-30ARP-B sensors embedded in the MWSs and the HMP45C-L sensor in the CCS. The sensor specifications are presented in Table 1.

TABLE 1. Technical specifications of the temperature and relative humidity sensors (SHT30-ARP-B) and Campbell Scientific station (HMP45C-L).

|             | Measurement range | Precision | Resolution |
|-------------|-------------------|-----------|------------|
| SHT30-ARP-B | -40°C to 125°C    | ±0.3°C    | 0.015°C    |
|             | 0%–100% UR        | ±3% UR    | 0.01% UR   |
| HMP45C-L    | -40°C to 60°C     | ±0.4°C    | *          |
|             | 0.8%–100% UR      | ±3% UR    | *          |

\* Not informed

For the analysis, the Tukey test was used at a confidence interval of 5%. Data from E1, E3, E5, E7, E11, E13, E15, E17, and E19 were compared with the CSS data to explore any statistical differences between the meteorological data and calculated  $ET_0$  results.

## RESULTS AND DISCUSSION

### Simulations

The ANN and ANFIS performances decreased as the amplitude of the added time-variant random noise increased. In other words,  $R^2$  decreased, and MAE and RMSE increased.

TABLE 2 summarizes the IS performance at determining  $ET_0$  from only  $R_s$ , T, and RH as the noise amplitude increased.  $U_2$  and the soil heat flux were not included.

TABLE 2. Statistical performance of ISs against  $ET_0$  calculated by using theFAO-56 PM method (Allen et al., 1998) at a confidence level of 95%. The meteorological variables used were the air temperature, relative humidity, and solar radiation. The wind speed and soil heat flux were not used.

| IS  | RN* | $R^2$ | MAE  | RMSE | IS    | RN* | $R^2$ | MAE  | RMSE |
|-----|-----|-------|------|------|-------|-----|-------|------|------|
| ANN | 0%  | 0.99  | 0.07 | 0.09 | ANFIS | 0%  | 0.99  | 0.08 | 0.10 |
|     | 5%  | 0.93  | 0.27 | 0.33 |       | 5%  | 0.90  | 0.31 | 0.41 |
|     | 10% | 0.80  | 0.47 | 0.57 |       | 10% | 0.72  | 0.54 | 0.68 |
|     | 40% | 0.22  | 0.92 | 1.13 |       | 40% | 0.27  | 0.89 | 1.10 |
|     | 80% | 0.10  | 0.98 | 1.21 |       | 80% | 0.00  | 1.04 | 2.18 |

\* RN – Random Noise

When the random noise was 0%, the developed IS showed better agreement with theFAO-56 PM method than the four temperature-based methods analyzed by Trajkovic (2005): the simplified PM (Allen et al., 1998), Hargreaves (Hargreaves & Samani, 1985), and Thornthwaite (Thornthwaite, 1948) methods and a radial basis function network. Similarly, the developed IS performed better than the results reported by Kumar et al. (2002). Note that the datasets and analysis locations of the studies were different. Therefore, it cannot be concluded that one system performed better than the others did.

Kişı (2006) observed that decreasing the number of meteorological variables used to estimate  $ET_0$  decreased the performance of the ANN. TABLE 3 presents the primary statistical data of the ANN performance when meteorological variables were removed as inputs. For each situation, the ANN was retrained. For example, in the case where  $U_2$  was suppressed, the ANN was trained and evaluated by using only T, RH, and  $R_s$ . In simulations where meteorological variables were eliminated, no error was inserted in the data from the automatic weather station.

TABLE 3. Statistical performance of the ANN compared with  $ET_0$  calculated by the FAO-56 PM method (Allen et al., 1998) at a 95% confidence level as different meteorological variables were removed as inputs.

| Eliminated data   | $R^2$ | MAE  | RMSE |
|-------------------|-------|------|------|
| None              | 1.00  | 0.04 | 0.05 |
| $U_2$             | 0.99  | 0.07 | 0.09 |
| $U_2$ + RH        | 0.97  | 0.20 | 0.25 |
| $U_2$ + RH + Temp | 0.96  | 0.26 | 0.32 |

The results showed that, when only  $R_s$  was used, the ANN could predict 96% of the daily evapotranspiration with MAE of  $0.26 \text{ mm day}^{-1}$ .

**Reference evapotranspiration**

FIGURE 7 shows the average  $ET_0$  calculated by the MWSs (blue line) and by the FAO-56 PM method from CSS data (red line) for the period of April 4–July 31, 2018. The standard deviation for  $ET_0$  estimation by the MWSs decreased until May 28, which is when the training of the EANN ended.

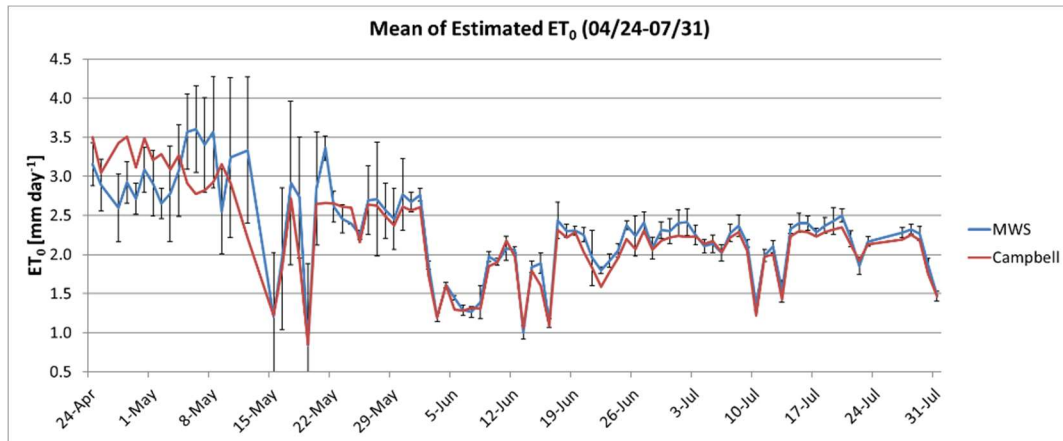


FIGURE 7. Daily evapotranspiration from April 24 to July 31, 2018 (blue line: average  $ET_0$  calculated by MWSs, red line:  $ET_0$  calculated with data from the CSS).

FIGURE 8 and FIGURE 9 visualize the evolution of the performance of the developed system with training.  $R^2$  of the linear regression model increased from 0.52 to 0.96 after the final learning.

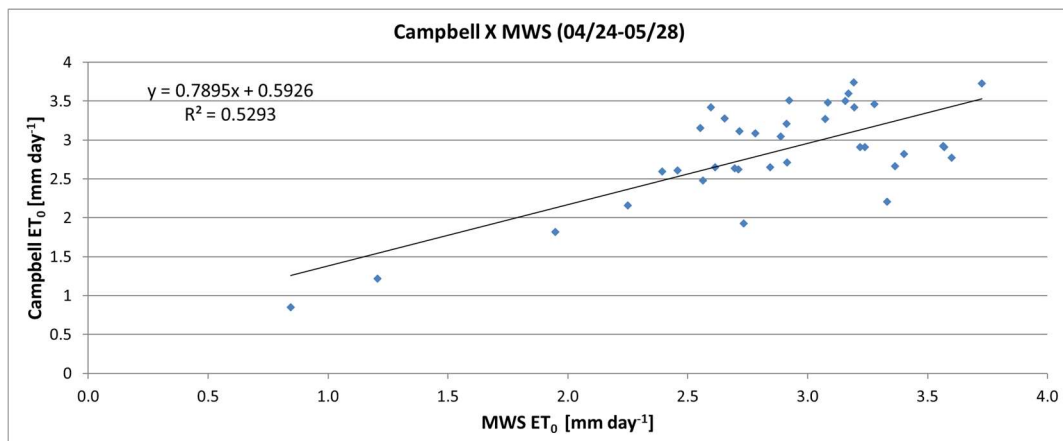


FIGURE 8. Correlation between the mean  $ET_0$  calculated by the MWSs and  $ET_0$  calculated with data from the CSS from April 4 to May 28, 2018.

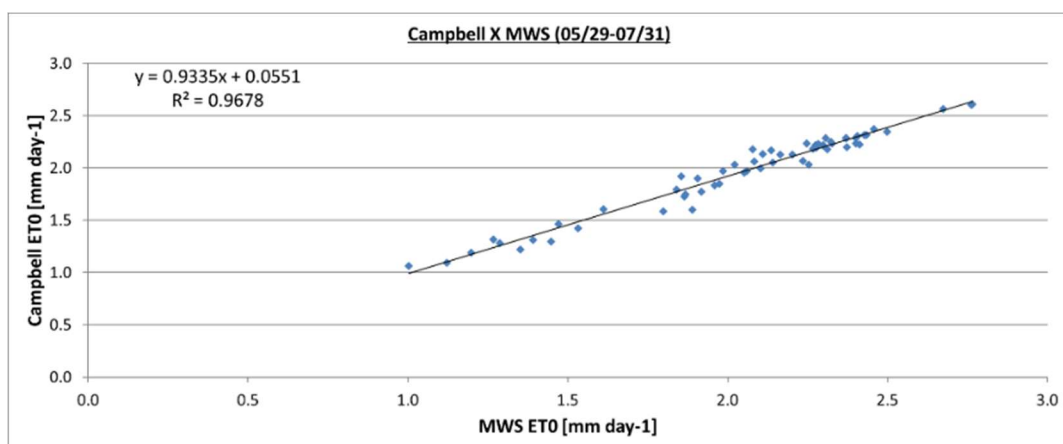


FIGURE 9. Correlation between the mean  $ET_0$  calculated by the MWSs and  $ET_0$  calculated with data from the CSS from May 29 to July 31, 2018.

Table 4 presents the main statistical parameters used to verify the agreement between the EANN and  $ET_0$  calculated with data from the CSS and using the FAO-56 PM equation for the period of April 24–July 31, 2018. The parameters for the training period (April 4–May 28) are in the upper part of the table. The lower part presents the same data but for the execution period (May 29–July 31). After the last training,  $R^2$  was 0.968, MAE was  $0.055 \text{ mm day}^{-1}$ , and RMSE was  $0.063 \text{ mm day}^{-1}$ .

TABLE 4. Main statistical parameters used to verify the agreement between the EANN and calculated  $ET_0$  for the period of April 4–July 31, 2018.

| Training (April 4–May 28)  |        |               |                         |
|----------------------------|--------|---------------|-------------------------|
|                            | Errors | F*            | P-Value                 |
| $\bar{\sigma}$             | 0.922  | 39.353        | $3.377 \times 10^{-7}$  |
| MAE                        | 0.090  | <b>a</b>      | <b>b</b>                |
| RMSE                       | 0.124  | 0.789         | 0.593                   |
| $R^2$                      | 0.529  | $y = a x + b$ |                         |
| $F_p^{**}$                 | 1.019  |               |                         |
| Execution (May 29–July 31) |        |               |                         |
|                            | Errors | F*            | P-Value                 |
| $\bar{\sigma}$             | 0.204  | 1772.641      | $1.018 \times 10^{-45}$ |
| MAE                        | 0.055  | <b>a</b>      | <b>b</b>                |
| RMSE                       | 0.063  | 0.934         | 0.055                   |
| $R^2$                      | 0.968  | $y = a x + b$ |                         |
| $F_p^{**}$                 | 1.041  |               |                         |

\*For a significance level (Alpha) of 0.05

\*\*Proportion factor between estimated and real  $ET_0$

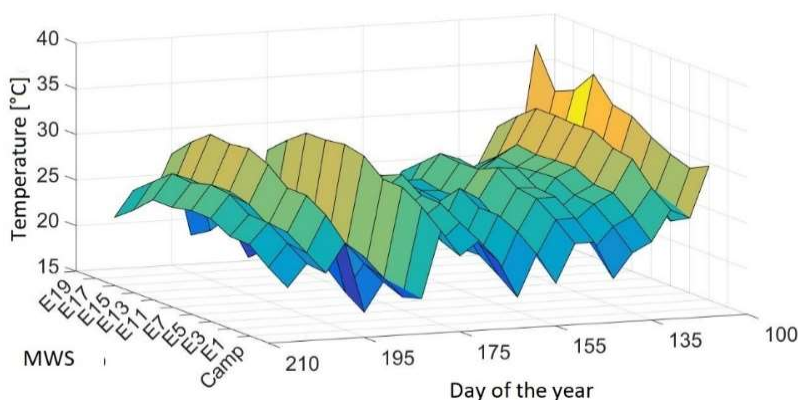
$\bar{\sigma}$  – Mean standard error

MAE – Mean absolute error

RMSE – Root mean squared error

### Climate variability

The Tukey test showed differences in the data among MWSs. The differences were greater for T than for RH. The differences among stations tended to be greater for data collected at 15-min intervals than at daily intervals. FIGURE 10 shows that T tended to increase for MWSs closer to the back of the greenhouse (i.e., east), which corresponded to E7–E13. However, this variation was not observed for RH. In other words, the greatest variation occurred along the east–west axis.



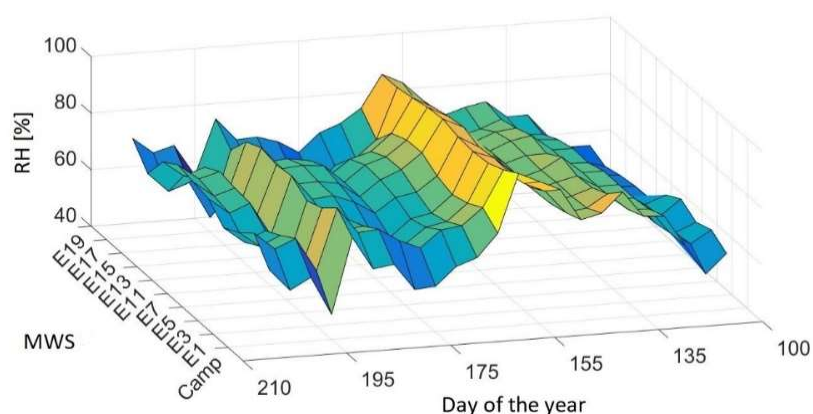


FIGURE 10. Distribution surfaces of the temperature (top) and relative humidity (bottom) in the greenhouse during the analysis period.

When the Tukey test was performed on  $ET_0$  calculated by MWSs with data from the period of May 29–July 31, 2018, no statistical differences were observed between stations. The lack of a statistical difference between  $ET_0$  values despite the difference in meteorological data can be explained by the training of the EANN to obtain the relationship between the meteorological data of each station and  $ET_0$  as calculated with the data from the CSS.

Li et al. (2017) analyzed the microclimatic variation of two greenhouses naturally ventilated and oriented east–west in Shouguang, China. They found that the greatest variation in T occurred along the east–west axis, followed by distance from the ground. Almost no variation was observed regarding the distance from the south wall of the greenhouse. They did not consider the variation in RH according to the sensor position in the greenhouse. Fatnassi et al. (2015) used computational fluid dynamics to simulate the distributions of  $R_s$  and T for two types of greenhouses with solar panels installed on the roof. The Venlo-type greenhouse showed less variation in T than the asymmetric-type greenhouse, and differences of greater than  $8^\circ\text{C}$  along the east–west axis and about  $6^\circ\text{C}$  along the north–south axis were observed. García-Ruiz et al. (2018) analyzed the heterogeneity of T inside a greenhouse in Almería, Spain, to verify worker safety as required by ISO 7726. They used a wireless sensor network that they previously developed for over a full year (December 2016–November 2017). The sensors were installed in a mesh of twelve nodes that were  $10\text{ m} \times 8\text{ m}$  apart from each other. Each node had three sensor elements at different heights (0.23, 0.93, and 1.56 m). They found that the greatest variation in T occurred in the horizontal direction, during the day, and along the east–west axis. Winter and summer had greater homogeneity. Vertical heterogeneity was greater in the colder seasons.

## CONCLUSIONS

The results of this work are in agreement with the previous studies and show that a low-cost IS can feasibly be applied to autonomous irrigation management, even if the available data are noisy and not all involved variables are available. The developed system can help minimize the impact of water shortages and small farmers participate in technological advances in agriculture. The major conclusions are as follows:

- ISs can estimate  $ET_0$  even with noisy data and without all meteorological variables needed for the FAO-56 PM method;
- Low-cost MWSs are a feasible approach for improving irrigation efficiency if combined with an IS;
- Despite differences in quality between the meteorological data from low-cost MWSs and a standard weather station, the developed IS can compute  $ET_0$  with the same level of accuracy.

## ACKNOWLEDGMENTS

The authors express their gratitude to FAPESP (São Paulo Research Foundation) for their financial support, under FAPESP Innovative Research in Small Business (PIPE), project: 2018/13090-1. They would also like to thank, USP (University of São Paulo) and DieTech Robotics and Automation Company for the technical support.

## REFERENCES

- Abioye EA, Abidin MSZ, Mahmud MSA, Buyamin S, Ishak MHI, Abd Rahman MKI, Ramli MS A (2020) A review on monitoring and advanced control strategies for precision irrigation. *Computers and Electronics in Agriculture* 173: 105441.
- Alavi N, Warland JS, Berg AA (2006) Filling gaps in evapotranspiration measurements for water budget studies: Evaluation of a Kalman filtering approach. *Agricultural and Forest Meteorology* 141(1): 57-66.
- Allen RG, Pereira LS, Raes D, Smith M (1998) Crop evapotranspiration-Guidelines for computing crop water requirements-FAO Irrigation and drainage paper 56. Fao, Rome, 300(9): D05109.
- Antonopoulos VZ, Antonopoulos AV (2017) Daily reference evapotranspiration estimates by artificial neural networks technique and empirical equations using limited input climate variables. In *Computers and Electronics in Agriculture* 132: 86-96.
- Bedi J (2022) Transfer learning augmented enhanced memory network models for reference evapotranspiration estimation. *Knowledge-Based Systems* 237:107717.

- Binfet J, Wilamowski BM (2001) Microprocessor implementation of fuzzy systems and neural networks. In Neural Networks. In: International Joint Conference on IEEE, Proceedings...
- Castell N, Dauge FR, Schneider P, Vogt M, Lerner U, Fishbain B, Bartonova A (2017) Can commercial low-cost sensor platforms contribute to air quality monitoring and exposure estimates? *Environment international* 99: 293-302.
- Curto A, Donaire-Gonzalez D, Barrera-Gómez J, Marshall JD, Nieuwenhuijsen MJ, Wellenius GA, Tonne C (2018) Performance of low-cost monitors to assess household air pollution *Environmental research* 163: 53-63.
- Fang Z, Wang Y, Peng L, Hong H (2021) Predicting flood susceptibility using LSTM neural networks. *Journal of Hydrology* 594: 125734.
- Fatnassi H, Poncet C, Brun R, Muller MM, Bertin N (2013) CFD study of climate conditions under greenhouses equipped with photovoltaic panels. *International Conference on Agricultural Engineering: New Technologies for Sustainable Agricultural Production and Food Security* 1054: 63-72.
- FAO & WWWC (2015) Towards a water and food secure future: critical perspectives for policy-makers. White Paper, FAO and World Water Council, Rome, Marseille.
- García-Ruiz RA, López-Martínez J, Blanco-Claraco JL, Pérez-Alonso J, Callejón-Ferre AJ (2018) On air temperature distribution and ISO 7726-defined heterogeneity inside a typical greenhouse in Almería. *Computers and electronics in agriculture* 151: 264-275.
- Gunawardena N, Pardyjak ER, Stoll R, Khadka A (2018) Development and evaluation of an open-source, low-cost distributed sensor network for environmental monitoring applications. *Measurement Science and Technology* 29(2): 024008.
- Guo J, He B, Sha Q (2018) Shallow-sea application of an intelligent fusion module for low-cost sensors in AUV *Ocean Engineering* 148: 386-400.
- Hargreaves GH, Samani ZA (1985) Reference crop evapotranspiration from temperature. *Applied Engineering in Agriculture* 1(2): 96-99.
- Instituto Brasileiro de Geografia e Estatística – IBGE (2009) Censo agropecuário – 2006 IBGE Rio de Janeiro.
- Jimenez AF, Cardenas PF, Canales A, Jimenez F, Portacio A (2020) A survey on intelligent agents and multi-agents for irrigation scheduling. *Computers and Electronics in Agriculture* 105474.
- Johnson NE, Bonczak B, Kontokosta CE (2018) Using a gradient boosting model to improve the performance of low-cost aerosol monitors in a dense, heterogeneous urban environment *Atmospheric Environment* 184: 9-16.
- Kişi Ö (2006) Generalized regression neural networks for evapotranspiration modeling. *Hydrological Sciences Journal* 51(6): 1092-1105.
- Kosko B (1994) Fuzzy systems as universal approximators. *IEEE transactions on computers* 43(11): 1329-1333.
- Kumar M, Raghuwanshi NS, Singh R, Wallender WW, Pruitt WO (2002) Estimating evapotranspiration using artificial neural network. *Journal of Irrigation and Drainage Engineering* 128(4): 224-233.
- Leal-Junior AG, Vargas-Valencia L, dos Santos WM, Schneider FB, Siqueira AA, Pontes MJ, Frizzera A (2018) POF-IMU sensor system: A fusion between inertial measurement units and POF sensors for low-cost and highly reliable systems. *Optical Fiber Technology* 43: 82-89.
- Li A, Huang L, Zhang T (2017) Field test and analysis of microclimate in naturally ventilated single-sloped greenhouses. *Energy and Buildings* 138: 479-489
- Lu H, Bryant RB, Buda AR, Collick AS, Folmar GJ, Kleinman PJ (2015) Long-term trends in climate and hydrology in an agricultural, headwater watershed of central Pennsylvania, USA. *Journal of Hydrology: Regional Studies* 4: 713-731.
- Oliveira GDL (2016) The geopolitics of Brazilian soybeans. *The Journal of Peasant Studies* 43(2): 348-372.
- Poggi S, Vinatier F, Hannachi M, Sanz Sanz E, Rudi G, Zamberletti P (2021) How can models foster the transition towards future agricultural landscapes. *The Future of Agricultural Landscapes*, In *Advances in Ecological Research Part II*, Academic Press, p305-368.
- Raj R, Mathew J, Kannath SK, Rajan J (2022) Crossover based technique for data augmentation. *Computer Methods and Programs in Biomedicine* 218: 106716.
- Sidhua RK, Kumara R, Ranaa PS, Jatb ML (2021) Automation in drip irrigation for enhancing water use efficiency in cereal systems of South Asia: Status and prospects. *Advances in Agronomy*, Academic Press, p247-300.
- Thornthwaite CW (1948) An approach toward a rational classification of climate. *Geographical review* 38(1): 55-94.
- Trajkovic S (2005) Temperature-based approaches for estimating reference evapotranspiration. *Journal of irrigation and drainage engineering* 131(4): 316-323.
- Yu S, Wang T, Wang J (2022) Data Augmentation by program transformation. *Journal of Systems and Software* 111304.
- Zhang CH, Benjamin WA, Miao WANG (2021) The contribution of cooperative irrigation scheme to poverty reduction in Tanzania. *Journal of Integrative Agriculture* 20(4): 953-963.